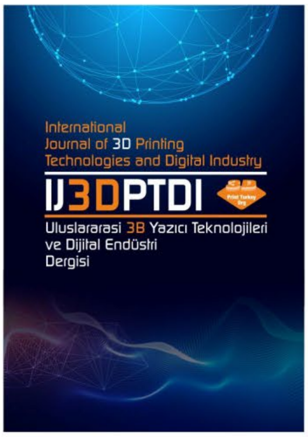

ULUSLARARASI 3B YAZICI TEKNOLOJİLERİ
VE DİJİTAL ENDÜSTRİ DERGİSİ

INTERNATIONAL JOURNAL OF 3D PRINTING TECHNOLOGIES AND DIGITAL INDUSTRY

ISSN:2602-3350 (Online)

URL: https://dergipark.org.tr/ij3dptdi

FABRICATION AND CHARACTERIZATION OF 3D PRINTED POLYMER OPTICAL WAVEGUIDES

Yazarlar (Authors): Kapil Kotadiya, Rachana Vokkekhur, Thomas Fuhrmann*

Bu makaleye şu şekilde atıfta bulunabilirsiniz (To cite to this article): *Kotadiya K., Vokkekhur R., Fuhrmann T., "Fabrication and Characterization of 3D Printed Polymer Optical Waveguides" Int. J. of 3D Printing Tech. Dig. Ind., 10(1): 01-10, (2026).*

DOI: 10.46519/ij3dptdi.1715513

Araştırma Makale/ Research Article

Erişim Linki: (To link to this article): https://dergipark.org.tr/en/pub/ij3dptdi/archive

FABRICATION AND CHARACTERIZATION OF 3D PRINTED POLYMER OPTICAL WAVEGUIDES

Kapil Kotadiya[a], Rachana Vokkekhur[a], Thomas Fuhrmann[b]*

[a]OTH Regensburg, Faculty of Applied Natural Sciences and Cultural Studies, Regensburg, Germany
[b]OTH Regensburg, Faculty of Electrical Engineering and Information Technology, Regensburg, Germany

* *Corresponding Author:* thomas.fuhrmann@oth-regensburg.de

(**Received:** 06.06.25; **Revised:** 08.01.26; **Accepted:** 23.02.26)

ABSTRACT

Polymer-based 3D printed optical waveguides are fabricated and characterized using a low-cost fused deposition modeling (FDM) printer. Waveguides with two different material combinations are printed: Polymethyl Methacrylate (PMMA) as core material with Polylactic Acid (PLA) as cladding material, and Polyethylene Terephthalate Glycol (PETG) as core material and PMMA as cladding material. Several waveguides with different printing parameters were produced and characterized. The adhesion between the filament lines is acceptable to good for both material combinations and all printing parameters with better adhesion for higher extrusion factors. The waveguide cross-sections were analyzed using an illuminating LED, a microscope lens, and a camera. The cross-sections of the waveguides with PMMA core and PLA cladding show fully illuminated core filaments and dark cladding filaments. Some waveguides with PETG core and PMMA cladding show dark core filaments and a high amount of light in the cladding. Air gaps between filament lines are seen in the cross-section analysis. They can be reduced but not fully eliminated by optimizing the printing parameters. The attenuation was analyzed with a cut-back method using an LED as a light transmitter, and a photodiode as a receiver. The waveguide attenuation is between 0.78 dB/cm and 1.50 dB/cm with no systematic differences for both material combinations. The highest attenuation is seen where the core is printed as one filament line. The results of these experiments show that 3D printing offers a viable method to produce optical waveguides that can be used as building blocks for optical components or optical sensors.

Keywords: Polymer Optics, 3D Printed Waveguide, Optical Waveguide Attenuation.

1. INTRODUCTION

Optical waveguides are used to transport light from one position to another. They can used for diverse applications, like telecommunication, material processing, sensing, and many more applications. Optical waveguides are typically made of two materials, the core with a higher refractive index where the light propagates, and the cladding with a lower refractive index to facilitate total internal reflection for light guidance. There are many known technologies to produce optical waveguides in different material systems, like glass, silicon, LiNbO3, and polymers [1].

3D printing is a generic term for many additive manufacturing technologies using different materials. Yousfi et al. showed that PLA and PMMA can be printed on each other with good cohesion between the layers [2]. Optical waveguides have been printed using diverse technologies. One possibility of 3D printing optical waveguides is using a common fused deposition modeling (FDM) printer, printing preforms, and then drawing optical fibers with differently shaped cores. Preforms with different shapes out of various materials have been produced and drawn to analyze distortions due to the drawing process and optimize it [3]. Zhao et al. utilized 3D printing to produce a preform and afterwards drew a fiber from it with Polycarbonate (PC) for the fiber core and Acrylonitrile-Butadiene-Styrene (ABS) for the cladding to produce multimode fibers with an attenuation range between 0.7 dB/cm and 1.8 dB/cm [4]. Microstructured optical fibers have been produced by directly extruding polymer with specially shaped nozzle and characterized by Talataisong et al. [5]. No layered filament 3D printing process has been used. The authors reached an attenuation of 1.1 dB/cm at a wavelength of λ_0=1557 nm.

Basar et al. propose a CO_2 laser cutting method to post-process 3D printed components using filaments [6]. Depending on the process parameters, a surface roughness better then 2 µm is achieved. Different mathematical models were compared regarding the accuracy of surface roughness prediction. Der et al. showed with a similar process technology a surface roughness below 1 µm [7].

Several extensive review articles were written to give an overview and summarize the production of optical components using 3D printing technologies. Blachowicz et al. review several technologies to print optical components, like lenses, mirrors, diffraction gratings, waveguides, and other parts [8]. The authors review many techniques using 3D printers to produce optical waveguides. Most of the waveguides have been produced using the print head as an extruder or printing a pre-form and drawing the waveguide. Gao et al. wrote an overview article about many different 3D printing techniques that can be used to produce diverse optical components [9]. Also in this overview, waveguide production technologies are shown that use the 3D printer as an extruder or for producing a pre-form. Zhu et al. describe various 3D printing technologies to produce optical components [10]. This article describes hollow core waveguides for THz waves and high-precision structures for optical waveguides. In all these three reviews, the focus is on high precision 3D printing technologies, but no versatile low-cost techniques are described for producing multimode waveguides for short distances.

Xu et al. give an extensive review on many diverse 3D printing technologies using functional polymers [11]. First, the authors review very many different printing technologies. The main focus is on incorporating functional nanoparticles into 3D printing to achieve new functionalities in diverse applications.

In the literature, no direct 3D printed optical waveguide using a standard and low-cost FDM printer was found. Therefore it was decided to research how to print waveguides, optimize the printing parameters, and characterize the cross-section and the attenuation. Two material combinations for the waveguides have been used. For the first waveguides, Polymethyl Methacrylate (PMMA) [12] for the core and Polylactic Acid (PLA) [13] for the cladding have been printed. The second waveguide material combination is Polyethylene Terephthalate Glycol (PETG) [14] for the core and PMMA for the cladding.

This research characterizing the fundamental parameters of 3D printed optical waveguides lays the foundation for many possible applications. Mechanical and optical component printing can be done together within one fabrication step, increasing functionality and reducing costs. Possible applications can be the integration of optical waveguides for communication, optical sensing of environmental parameters, sensors for user interaction, and light guides for optical indicators. The principles and implementations of these optical components are already known, but they are normally produced as separate components, resulting in higher costs and difficult integration into the system. It is therefore advantageous to develop integrated mechanical-optical parts with high functionality at low cost. Based on this 3D printing technology, an optical position sensor was developed and characterized in this research group [15].

Section 2 describes the process of waveguide fabrication. The waveguides are measured using a microscope lens and a camera; the results are shown in Section 3. The attenuation measurements of all waveguides are listed in Section 4. The results are summarized and conclusions are drawn in Section 5.

2. WAVEGUIDE FABRICATION

2.1. Materials for Waveguides

The polymer materials for the core and the cladding of the waveguide have been chosen so that the core material has a higher refractive than the cladding material to ensure total internal reflection for guided waves. There are no refractive index data of the filaments from the manufacturers. Therefore, refractive index data have been taken from the literature [16]. The refractive index data are at a wavelength of λ_0=635 nm, as the LED has a central wavelength between λ_{LEDmin}=630 nm and λ_{LEDmax}=685 nm. The refractive index data for PET has been taken instead of the data for PETG, as no profound PETG data has been found and the two materials have very similar chemical structures and properties. The minimal refractive index differences between PET and PETG according to [17] are not relevant in these multimode waveguides.

The refractive index parameters for the first material combination are:

- Core: PMMA, refractive index n_{PMMA}=1.4905,
- Cladding: PLA, refractive index n_{PLA}=1.4507.
-

This results in a numerical aperture of the waveguide of NA_1=0.342 equal to a maximal acceptance angle of θ_1=20.0°. This equals to a theoretical bandwidth-length product for optical communication of 7.34 GHz·m.

The refractive index parameters for the second material combination are:

- Core: PETG, refractive index n_{PETG}=1.5650,
- Cladding: PMMA, refractive index n_{PMMA}=1.4905.

This results in a numerical aperture of the waveguide of NA_2=0.477 equal to a maximal acceptance angle of θ_2=28.5°. This equals to a theoretical bandwidth-length product for optical communication of 3.84 GHz·m.

These numerical apertures and acceptance angles are in the range of typical values for optical multi-mode fibers. This results in a good guidance of the light in the core.

2.2. 3D Printing

It was decided to print all waveguides on a PRUSA MK3 [18] with a filament changing unit. The nozzle diameter is 0.4 mm. The fan of the 3D printer is switched off for all prints. The goal is that the filament cools down slower and has more time to connect with neighboring filament lines.

The overall height by overall width of the core is 1 mm by 1 mm and the total waveguide cross section is 2 mm by 2 mm. These dimensions have been chosen to be similar to standard polymer optical fibers (POFs) [19] with a core diameter of 980 µm and an outer diameter of 2.2 mm, so a standard LED [20] can be used as a light source.

Table 1. 3D Printed Polymer-Optical Waveguide Parameters.

Waveguide							3D Printer Properties						
Name	Core			Cladding			Nozzle Temp. in °C		Bed Temp. in °C		Print Speed in mm/s		Extrusion Factor
	Material	Height in mm	Width in mm	Material	Height in mm	Width in mm	Core	Clad.	Core	Clad.	Core	Clad.	
PW1	PMMA	0.25	0.5	PLA	0.25	0.5	255	205	110	60	25	25	1.05
PW2	PETG	0.25	0.5	PMMA	0.25	0.5	250	250	70	70	25	25	1.05
PW3	PMMA	0.25	0.5	PLA	0.25	0.5	250	215	70	60	20	20	1.10
PW4	PETG	0.25	0.5	PMMA	0.25	0.5	250	250	70	70	20	20	1.10
PW5	PMMA	0.25	0.5	PLA	0.25	0.5	250	230	70	70	20	20	1.0
PW6	PETG	0.25	0.5	PMMA	0.25	0.5	250	250	70	70	20	20	1.0
PW7	PMMA	0.25	1	PLA	0.25	0.5	250	230	70	70	20	20	1.05
PW8	PETG	0.25	1	PMMA	0.25	0.5	250	250	90	90	20	20	1.05
PW9	PMMA	1	1	PLA	0.25	0.5	250	230	70	70	2.5	20	1.05
PW10	PETG	1	1	PMMA	0.25	0.5	250	250	90	90	2.5	20	1.05

Ten types of waveguides with different printing parameters have been printed and characterized. This has been done in five iterations. After each iteration, the waveguides have been inspected and measured to improve the printing parameters for the next iteration. The main waveguide parameters are listed in Table 1. These waveguides are named PW1 to PW10.

The left side shows the waveguide parameters of the core and cladding, especially the materials and dimensions of the filament lines. The right side of the table shows the parameters of the 3D printer, especially the temperatures, the printing speed, and the extrusion factor compared to the nominally extruded amount of material. The nozzle and bed temperatures were chosen according to the data sheets and printer recommendations. The print speed was chosen much slower than the usual print speed so the polymer has time to fill gaps and connect with previous layers. All waveguides with odd numbers are printed with a PMMA core and PLA cladding; the waveguides with even numbers are printed with a PETG core and a PMMA cladding.

Waveguides PW1 and PW2 have been printed with an initial set of parameters without any experience in optimizing the waveguide printing. The standard height of 0.25 mm and the standard width of 0.5 mm of each filament line has been chosen. The nozzle and bed temperatures have been chosen according to filament data sheets.

For waveguides PW3 and PW4, the extrusion factor of the filament has been increased to press more filament into the air gaps between the filament lines, and therefore reduce the amount of air between the filament lines.

Waveguides PW5 and PW6 have been printed with a reduced amount of filament, and the standard extrusion factor of 1.0 is chosen.

For the PW7 and PW8 waveguides, the core has been printed in four layers, each with 1 mm by 0.25 mm. In each layer, the cladding has been printed first, followed by the core. The goal of this variant is to eliminate the air gaps between adjacent core layers to have a homogeneous core.

For waveguides PW9 and PW10, the cladding layers until the full height of the core have been printed first. Afterward, the core has been printed in the dimensions of 1 mm by 1 mm so that the nozzle disperses the core material in one filament line. The idea behind this structure is that the core is built from one homogeneous filament line without interfaces between core filament lines and air gaps.

All material combinations have acceptable to good adhesion between adjacent filament lines. Visual inspection showed no separation of filament lines after printing. Waveguide bending has not been observed after printing and cooling down.

2.3. Cutting, Grinding, and Polishing

After printing the waveguides, approximately 5 mm of the waveguide length at the end faces are not homogeneous, as there is the start and stop point of printing and also the print head turns when printing several lines without interruptions. The first step of waveguide preparation for measurement is therefore to cut the two ends of the polymer optical waveguide by 1 cm to remove the part that is not evenly printed. A multi-tool, DREMEL® 4250 (4250-35) [21] with a diamond blade [22] is used to cut the polymer optical waveguide without applying mechanical pressure.

The next step is to grind and polish both ends of the waveguide with different grinding and polishing papers to get rectangular surfaces, eliminate the scratches, and achieve smooth and even surfaces. Fig. 1 shows the waveguide that is inserted into a self-build holder for a rectangular angle and a constant contact pressure, and also the four grinding and polishing papers from rough to fine can be seen. All of the polishing is done by hand, using this mechanical holder and performing figure-eight polishing patterns to get the surface homogeneously polished in all directions, as can be seen in Fig. 1.

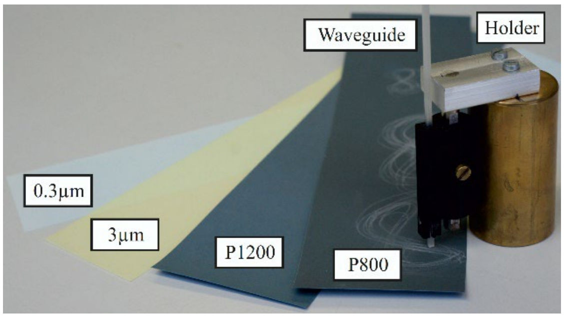

Figure 1. Polishing Setup and Polishing Papers.

First, a silicon carbide sandpaper [23] with P800 grit is used for dry-grinding the waveguide to make the surface rectangular and even. Second, a silicon carbide sandpaper with P1200 grit is used for dry-grinding the waveguide, to make the surface smooth. Third, two polishing papers with 3 µm grit [24] and afterward with 0.3 µm grit [25] are used for wet-polishing the polymer optical waveguide to remove scratches and achieve a smooth surface. The reason to achieve the smooth surface by polishing is to reduce the stray light out of the printed waveguide that would lead to additional losses of the coupling between the waveguide and the photodiode. This would affect the accuracy of the attenuation measurements.

The inspection of the surface is done by using a microscope lens and a camera. This is the same setup as it is used to evaluate the waveguide cross-section in Section 3 and can be seen in Fig. 2.

3. WAVEGUIDE CROSS-SECTION INSPECTIONS

3.1. Inspection Goals

The first goal of the waveguide cross-section inspections is to see the printing quality of the filaments. As the end of the waveguide is cut by 1 cm, the homogeneous region of the waveguide is inspected and it is assumed that the cross-section of the whole waveguide is identical to the documented cross-section.

The second goals is to see the light distribution inside the waveguide, if the light is inside the core and the cladding is dark. Therefore, the waveguide was illuminated from the backside by a LED.

3.2. Inspection Setup

For inspecting the waveguide cross-sections, as shown in Fig. 2, the following instruments are used:

- Polymer Optical Waveguide (PW1 to PW10),
- Red LED [20],
- Lens: Carl Zeiss Epiplan 4/0.1,
- Camera: Thor Digital Camera (CS165MU/M) [26],
- Tube length: 12 cm,
- DC power source: RIGOL DP831 [27],
- Diverse mounts on an optical table.

A red LED [20] is attached to the polymer optical waveguide and is connected to a DC power source [27]. The polymer optical waveguide is held by a support in front of the microscope lens with the camera setup. The lens is attached to a black-and-white camera using a tube with a length of 12 cm. All components are mounted on an optical table. The camera is connected to a computer and ThorCam software is used to inspect the surface of the waveguide and record the observations. The setup can be seen in Fig. 2. The waveguide is shining red. On the first centimeters, the main reason is the light in the cladding from the LED to waveguide coupling. The waveguide glowing afterward is stray light due to core material inhomogeneities, and imperfections between core and cladding.

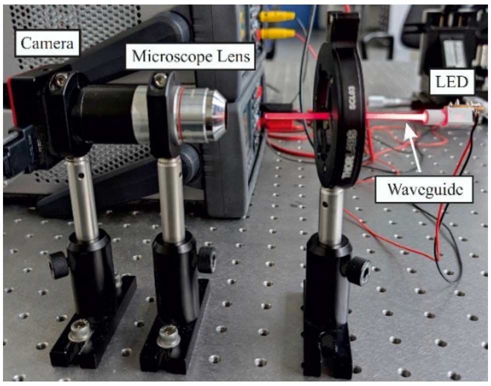

Figure 2. Waveguide Cross-Section Inspection Setup.

3.3. Inspection Results

The images in Fig. 3, Fig. 4, Fig. 5, Fig. 6, and Fig. 7 are captured with the setup that is shown in Fig. 2. All waveguides in the Figures are so oriented that the first printed layer is at the bottom of the pictures. The properties of the corresponding polymer optical waveguides can be seen in Table 1. All waveguides have nominal core dimensions of 1 mm by 1 mm and total waveguide dimensions of 2 mm by 2 mm. Fig. 3 shows the cross-section measurements of the initial 3D waveguide print. Printing parameters have been chosen according to data sheets and own thoughts. The left side shows the waveguide with PMMA as core material and PLA as cladding material (PW1). The total air void between the core filament layers is 0.78%. All core filaments are lit while all cladding filaments appear dark, The right side shows the waveguide with the PETG and PMMA combination (PW2). The total air void between the core filament layers is 0.61%. The lowest core layer is nearly dark. It looks like an optical intersection with different refractive indices has been produced during the printing process. The exact reason for this effect is unclear.

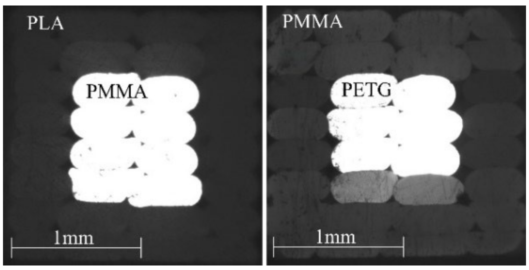

Figure 3. Waveguide Cross-Section Images: left: PW1, right:PW2.

The waveguides PW3 and PW4 are seen in Fig. 4. The amount of polymer is increased by giving a higher extrusion factor (see Table 1) to reduce the air gaps between the filament lines. This was partly successful as the air gaps were reduced to 0.39% on the left image and 0.41% on the right image, but not fully disappeared. It is good to see that the printing sequence is optimized by the slicing software for a minimal number of filament changes. Therefore, the printing sequence between the core and cladding is reversed for subsequent layers. This results in an asymmetric waveguide cross-section.

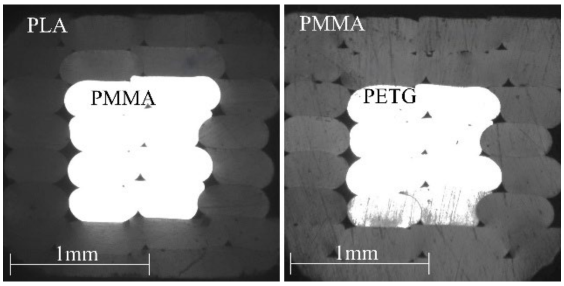

Figure 4. Waveguide Cross-Section Images: left: PW3, right: PW4.

The waveguides PW5 and PW6 in Fig. 5 have reduced amounts of filament. It can be seen that there are large air gaps between the core layers of 1.7% on the left image and 1.6% on the right image, and there are also air gaps between the core and cladding. Some of the core filament layers have no contact with the cladding filament. This changes the light guiding properties and reduces the mechanical strength of the waveguide. From the Figures it can be seen that there is more stray light in the cladding of PW6 than of PW5. Some of the test waveguides showed a delamination between the filament lines after cutting and grinding the waveguides. This is due to the low adhesion area between the filament lines due to the air gaps. Waveguides with higher extrusion factors don't show this delamination tendency.

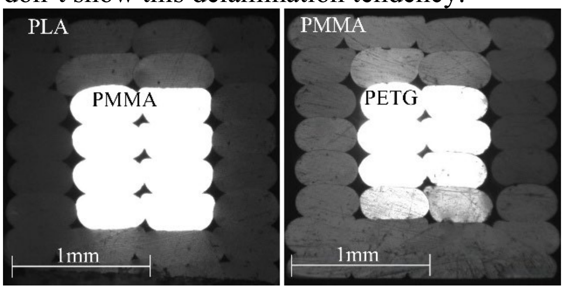

Figure 5. Waveguide Cross-Section Images: left: PW5, right: PW6.

Fig. 6 shows PW7 and PW8 where the dimensions of the filament printing have been changed. Each core layer is printed as one filament line with dimensions of 1mm by 0.25 mm. For each layer, the cladding has been printed before the core. It is good to see that the core has no air gaps in-between and also the air gaps between the core and cladding are small. It can be seen that there is a low amount of stray light in the first upper cladding layer of PW7.

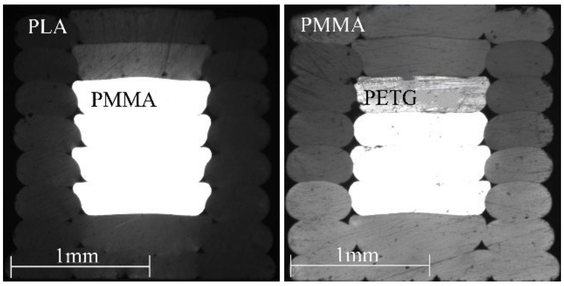

Figure 6. Waveguide Cross-Section Images: left: PW7, right:PW8.

The last waveguide variant is shown in Fig. 7. The four cladding layers that form the side walls of the core have been printed first. The complete core was printed as one filament line afterward. It was tested if a big core can be printed with a 0.4 mm nozzle. In PW10, the upper cladding layer looks like there are some air gaps between the filament lines. The pictures also show that PW10 has more stray light in the cladding than PW9.

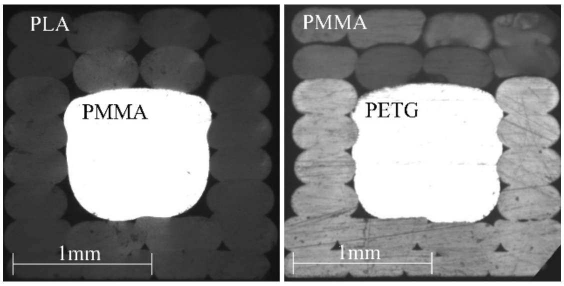

Figure 7. Waveguide Cross-Section Images: left: PW9, right: PW10.

When checking the surface qualities in Fig. 3 to Fig. 7, slight scratches can be seen. This leads to the conclusion that there is a small amount of stray light due to the surface scratches. Therefore, a photodiode with a large area has been chosen and it was placed directly at the waveguide surface. Also stray light from the waveguide has been detected by the photodiode.

4. ATTENUATION MEASUREMENTS

4.1. Measurement Setup and Process

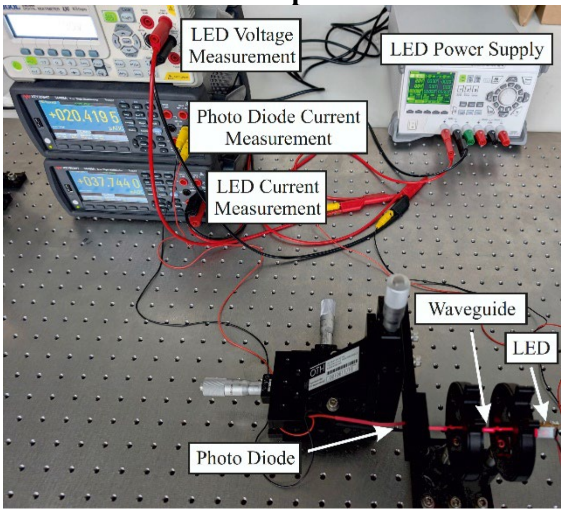

Figure 8. Attenuation Measurement Setup.

The attenuation measurement setup can be seen in Fig. 8. It consists of the following parts:

- A 3D printed, polished, polymer optical waveguide.
- Red LED light source [20] attached to the polymer optical waveguide.
- DC power source RIGOL DP831 [27] to supply current to the LED.
- Photodiode [28] with 21 mm^2 active area to receive all light from the printed waveguide independent of the outcoupling angle.
- Two Keysight 34465A Multi-meters [29] to measure the LED current and the current received by the photodiode.
- One Digital Multimeter Rigol DM3068 to measure the LED voltage [30].

The LED is fixed to the waveguide and is connected to a programmable electrical current source. Two electric multimeters are connected to the LED to measure voltage and current. The photodiode is fixed on the optical table with a distance of approximately 1mm to the other end of the waveguide and is connected to a multimeter with a current sensitivity of 1 pA for measuring the output current. The measurement process is performed under low-light conditions to avoid a measurement offset caused by ambient stray light.

For measuring the attenuation of the polymer optical waveguide in dB/cm, the cut-back method is used. This is a standard method to measure the attenuation of optical waveguides by cutting back the structure by defined distances and measure the attenuations. The attenuations are measured and set in relation to the optical waveguide length to determine the attenuation in dB/cm. The main advantage is that there are many attenuation measurements possible to reduce measurement errors. The main disadvantage is the destructive nature of this measurement principle [31].

After every measurement, this polymer waveguide is cut by approximately 1 cm, and the polishing process for the polymer optical waveguide is repeated after every cut. To ensure the accuracy of the measurements and to eliminate measurement errors due to changes of the light source to waveguide coupling, the LED is kept attached to the waveguide throughout all measurements of a particular waveguide.

The nominal supply current for the LED has the same value for all measurements. As the current slightly fluctuates from measurement to measurement, it was corrected in the attenuation calculations (see (1)).

The attenuation is calculated as:

$$\alpha_n = 10 \cdot \log_{10}\left(\frac{I_{LEDn}}{I_{PDn}}\right) dB \quad (1)$$

The α_n in (1) is the attenuation of the whole optical system from the supplying LED current I_{LEDn} to the photodiode current I_{PDn}.

This results in an attenuation of the waveguide per length unit:

$$\alpha_{dB/cm} = \frac{\alpha_1 - \alpha_2}{L_1 - L_2} \quad (2)$$

In (2), $\alpha_{dB/cm}$ represents the attenuation coefficient in dB/cm, L_1 denotes the initial length of the optical fiber in cm, L_2 signifies the final length of the optical fiber after attenuation in cm. α_1 stands for the optical attenuation between the LED current and the photodiode current at fiber length L_1, and α_2 represents optical attenuation for fiber length L_2.

4.2. Attenuation Results

Table 2 shows the results of the attenuation measurements of the polymer optical waveguides. The first column shows the waveguide number. Nine measurements have been taken for each waveguide using the cut-back attenuation measurement principle. The average attenuation of all measurements and the standard deviations are shown in the right columns of Table 2.

The waveguide attenuation is between 0.78 dB/cm and 1.50 dB/cm. The standard deviation is ranging from 0.17 dB/cm to 0.60 dB/cm.

It is clear to see that there is no significant attenuation difference between the two material systems. The waveguides with the odd numbers with a PMMA core and a PLA cladding show a very similar attenuation behavior as the waveguides with the even numbers with a PETG core and a PMMA cladding.

Table 2. Waveguide Attenuation.

Name	Attenuation α in dB/cm										
	Meas. 1	**Meas. 2**	**Meas. 3**	**Meas. 4**	**Meas. 5**	**Meas. 6**	**Meas. 7**	**Meas. 8**	**Meas. 9**	**Average**	**Std. Dev.**
PW1	0.9	0.8	1.0	0.1	1.1	0.7	1.2	1.2	1.1	0.99	0.18
PW2	0.4	1.1	0.7	0.6	0.7	0.9	1.1	0.9	0.9	0.81	0.23
PW3	0.5	0.8	0.8	0.8	0.5	0.7	0.8	1.1	0.9	0.78	0.18
PW4	0.8	1.2	1.2	0.9	1.4	1.1	1.1	1.1	1.0	1.09	0.17
PW5	1.6	1.2	1.9	0.3	0.1	0.9	1.3	0.9	1.4	1.07	0.60
PW6	0.9	1.7	1.1	0.9	0.8	1.5	0.8	0.8	1.0	1.06	0.31
PW7	1.0	1.2	1.1	1.3	1.0	0.8	1.5	0.9	0.9	1.08	0.25
PW8	1.1	1.1	1.8	1.3	1.0	0.8	1.4	1.1	0.9	1.16	0.30
PW9	1.5	0.8	1.6	1.5	1.4	1.2	2.2	0.8	2.5	1.50	0.56
PW10	1.2	1.5	1.6	1.1	1.0	1.1	1.2	1.5	1.6	1.30	0.24

It is also good to see that the waveguide printing parameters have no significant influence on waveguide attenuation. Different printing speeds, core/cladding layer sequencing, different nozzle temperatures, and different extrusion factors (see Table 1) influence the mechanical properties of the waveguide but not the optical properties. The only exception are waveguides PW9 and PW10 with a significantly higher attenuation of 1.50 dB/cm and 1.30 dB/cm compared to the other waveguides. These waveguides have been printed with a core as a single filament line (see Fig. 7). The reason for this higher waveguide attenuation is unclear.

In sum, the waveguide attenuation for most configurations is approximately 1 dB/cm. This is a similar value to the research results of other authors [4, 5].

5. SUMMARY AND CONCLUSION

Polymer optical waveguides have been 3D printed with a filament printer using two material combinations and five different sets of printing parameters. Air gaps between filament lines with different sizes have been observed for all material combinations and all printing parameters. No severe adhesion problems between adjacent filaments have been seen. The adhesion is better for smaller air gaps that result from a higher extrusion factor. The waveguide is strait also after cooling down from the printing process. The waveguides were easy to cut using a diamond blade and were easy to grind and polish. The surface quality after polishing was good with a low number of small scratches.

All waveguides show an acceptable optical attenuation between 0.78 dB/cm and 1.50 dB/cm which is similar to other attenuation measurements that can be found in literature. This attenuation is caused mainly by material absorption and stray light due to printing imperfections.

All waveguides with PMMA core and PLA cladding show that the light is traveling in all core filaments, and nearly no light is traveling in the cladding filaments as theoretically expected. Some of the waveguides with PETG core and PMMA cladding show some core filaments where only little light is traveling, and light in the cladding filaments. The reason for this behavior is unknown.

In sum, both material combination and all printing parameters are suited for producing optical waveguides with an acceptable attenuation. The optical behavior of the waveguides with PMMA core and PLA cladding is slightly better as the core is more homogeneously illuminated and the stray light in the cladding is lower. This principal investigation of the 3D printed waveguides is very encouraging to use this technology basis for producing integrated optical-mechanical systems, like more complex waveguide structures, environmental sensing systems, sensors for user interaction, light indicators, and short-range optical communication systems up to 10Gbit/s. It is proven that this process technique works to produce low-cost optical waveguides with an acceptable optical attenuation and good mechanical properties. Based on these results, the research group is currently designing, producing, and characterizing more complex parts and systems.

ACKNOWLEDGES
The authors would like to thank the following people from OTH Regensburg. Dr. Heiko Unold from the Faculty of Electrical Engineering and Information Technology for the support with optomechanic measurement equipment. Michael Farmbauer and Florian Hollnberger for supporting the waveguide printing. Peter Fendrich from the Mechanical Workshop for making the polishing fixture.

REFERENCES
1. Selvaraja, S.K. and Sethi, P., "Review on optical waveguides", Emerging Waveguide Technology, Vol. 95, Page 458, 2018.

2. Yousfi, M., Belhadj, A., Lamnawar, K. and Maazouz, A., “3D printing of PLA and PMMA multilayered model polymers: An innovative approach for a better-controlled pellet multi-extrusion process”, ESAFORM 2021, 24th International Conference on Material Forming, Liège, Belgium, 2021.

3. Toal, P.M., Holmes, L.J., Rodriguez, R.X. and Wetzel, E.D., “Microstructured monofilament via thermal drawing of additively manufactured preforms”, Additive Manufacturing, Vol. 16, Pages 12-23, 2017.

4. Zhao, Q., Tian, F., Yang, X., Li, S., Zhang, J., Zhu, X., Yang, J., Liu, Z, Yuan, T. and Yuan, L., “Optical fibers with special shaped cores drawn from 3D printed preforms”, Optik, Vol. 133, Pages 60-65, 2017.

5. Talataisong, W., Ismaeel, R., Sandoghchi, S.R., Rutirawut, T., Topley, G., Beresna, M. and Brambilla, G., “Novel method for manufacturing optical fiber: extrusion and drawing of microstructured polymer optical fibers from a 3D printer”, Optics Express, Vol, 26, Issue 24, Pages 32007-32013, 2018.

6. Basar, G., Der, O., Guvenc, M.A., “AI-powered hybrid metaheuristic optimization for predicting surface roughness and kerf width in CO2 laser cutting of 3D-printed PLA-CF composites”, Journal of Thermoplastic Composite Materials, Vol. 38, Issue 7, Pages 2688-2717, 2025.

7. Der, O., Basar, G., “Investigation of the Effects of Process Parameters on Machining Performance in Laser Cutting of 3D-Printed PLA”, International Journal of 3D Printing Technology and Digital Industry,Vol. 9, Issue 1, Pages 9-20, 2025.

8. Blachowicz, T., Ehrmann, G. and Ehrmann, A., “Optical elements from 3D printed polymers”, e-Polymers, Vol. 21, Pages 549-565, 2021.

9. Gao, H., An, J., Chua, C.K., Bourell, D., ‘Kuo, C.-N. and Tan, D.T.H., “3D printed optics and photonics: Processes, materials and applications”, Materials Today, Vol. 69, Pages 107-132, 2023.

10. Zhu, Y., Tang, T., Zhao, S., Joralmon, D., Poit, Z., Ahire, B., Keshav, S., Raje, A.R., Blair, J., Zhang, Z. and Li, X., “Recent advancements and applications in 3D printing of functional optics”, Additive Manufacturing, Vol. 52, 102682, 2022.

11. Xu, W., Jambhulkar, S., Zhu, Y., Ravichandran, D., Kakarla, M., Vernon, B., Lott, D.G., Cornella, J.L., Shefi, O., Miquelard-Garnier, G., Yang, Y., Song, K., “3D printing for polymer/particle-based processing: A review”, Composites Part B: Engineering 223, 109102, 2021.

12. Material4Print, “PMMA Material Data Sheet”, https://www.material4print.de/media/pdf/be/0a/7e/Data_Sheet_M4P_PMMA.pdf, May 28, 2025.

13. BASF, “Ultrafuse PLA Technical Data Sheet”, https://move.forward-am.com/hubfs/AES Documentation/Standard Filaments/PLA/TDS/Ultrafuse_PLA_TDS_DE_v4.4.pdf, May 28, 2025.

14. Material4Print, “PETG Material Data Sheet”, https://www.material4print.de/media/pdf/79/b3/e5/Data_Sheet_M4P_PETG.pdf, May 28, 2025.

15. Zhong, G., “Calibration and Performance Evaluation of Contactless Optical Position Sensors Based on 3D Printed Optical Waveguides”, Bachelor Thesis, https://doi.org/10.35096/othr/pub-8466, August 12, 2025.

16. Polyanskiy, M., “Refractive index database”, https://refractiveindex.info, May 28, 2025.

17. El-Farahaty, K.A, Sadik, A.M. and Hezma, A.M, “Study of Optical and Structure Properties of Polyester (PET) and Copolyester (PETG) Fibers by Interferometry”, International Journal of Polymeric Materials, Vol. 56, Pages 715-728, 2007.

18. Prusa, “Original Prusa i3 MK3S+ 3D printer MMU3 kit”, https://www.prusa3d.com/de/kategorie/original-prusa-mmu3/, May 28, 2025.

19. Broadcom, “Plastic Fiber Cable”, https://www.broadcom.com/products/fiber-optic-modules-components/industrial/eval-kits-accessories/cables/hfbr-rus100z, May 28, 2025.

20. Broadcom, “SFH757 and SFH757V Data Sheet”, https://docs.broadcom.com/doc/AV02-2597EN, May 28, 2025.

21. Dremel, “Multifunktionswerkzeuge DREMEL 4250”, https://www.dremel.com/de/de/p/dremel-4250-f0134250ja, May 28, 2025.

22. Dremel, “SpeedClic: Diamant-Trennscheibe. (SC545)”, https://www.dremel.com/de/de/p/dremel-ez-speedclic-diamant-trennscheibe-2615s545jb, May 28, 2025.

23. Lanhu, “Lanhu 320 to 5000 Assorted Grain Sandpaper, 23 x 9 cm”, https://www.amazon.de/-/en/Lanhu-5000-Assorted-Grain-Sandpaper/dp/B08J7FY5RF, May 28, 2025.

24. Thorlabs, “LF3P - 11” x 9” Aluminum Oxide Lapping (Polishing) Sheets, 3 µm Grit”, https://www.thorlabs.de/thorproduct.cfm?partnumber=LF3P, May 28, 2025.

25. Thorlabs, “LF03P - 11” x 9” Calcined Alumina Lapping (Polishing) Sheets, 0.3 µm Grit”, https://www.thorlabs.de/thorproduct.cfm?partnumber=LF03P, May 28, 2025.

26. Thorlabs, “CS165MU/M - Zelux® 1.6 MP Monochrome CMOS Camera”, https://www.thorlabs.com/thorproduct.cfm?partnumber=CS165MU/M, May 28, 2025.

27. Rigol, “DP800 Series Programmable Linear DC Power Supply”, https://www.rigolna.com/products/dc-power-loads/dp800/, May 28, 2025.

28. Excelitas, “Photodiode VTP4085H-ND”, https://www.excelitas.com/product/vtp4085h-si-pd-ceramic-21mm2, May 28, 2025.

29. Keysight, “34465A 6.5 Digit Truevolt Digital Multimeter”, https://www.keysight.com/zz/en/product/34465A/digital-multimeter-6-5-digit-truevolt-dmm.html, May 28, 2025.

30. Rigol, “Digital Multimeter DM3068 Series”, https://int.rigol.com/products/DM_Detail/DM3068, May 28, 2025.

31. Ding, M., Fan, D., Wang, W., Luo, Y. and Peng, G.D., “Basics of Optical Fiber Measurements”, In: Peng, GD. editors Handbook of Optical Fibers, Page 18, Springer, Singapore, 2018.